water

MDPI

Article

Dimercaptosuccinic Acid Functionalized Polystyrene Column for Trace Concentration Determination of Heavy Metal Ions: Experimental and Theoretical Calculation Studies

Uzma Haseen [1], Syed Ghazanfar Ali [2], Khalid Umar [3,*], Abuzer Ali [4], Hilal Ahmad [5,6,*] and Haris Manzoor Khan [2]

1 Department of Chemistry, Faculty of Science, Aligarh Muslim University, Aligarh 202002, India; uzma.haseen@gmail.com
2 Department of Microbiology, Jawaharlal Nehru Medical College and Hospital, Aligarh Muslim University, Aligarh 202002, India; syedmicro72@gmail.com (S.G.A.); harismk2003@hotmail.com (H.M.K.)
3 School of Chemical Sciences, Universiti Sains Malaysia, Pulau Pinang 11800, Malaysia
4 Department of Pharmacognosy, College of Pharmacy, Taif University, P.O. Box 11099, Taif 21944, Saudi Arabia; abuali@tu.edu.sa
5 Division of Computational Physics, Institute for Computational Science, Ton Duc Thang University, Ho Chi Minh City 10000, Vietnam
6 Faculty of Applied Sciences, Ton Duc Thang University, Ho Chi Minh City 10000, Vietnam
* Correspondence: khalidumar4@gmail.com (K.U.); hilalahmad@tdtu.edu.vn (H.A.)

check for updates

Citation: Haseen, U.; Ali, S.G.; Umar, K.; Ali, A.; Ahmad, H.; Khan, H.M. Dimercaptosuccinic Acid Functionalized Polystyrene Column for Trace Concentration Determination of Heavy Metal Ions: Experimental and Theoretical Calculation Studies. *Water* **2021**, *13*, 3056. https://doi.org/10.3390/w13213056

Academic Editor: David Widory

Received: 28 September 2021
Accepted: 27 October 2021
Published: 1 November 2021

Publisher's Note: MDPI stays neutral with regard to jurisdictional claims in published maps and institutional affiliations.

Copyright: © 2021 by the authors. Licensee MDPI, Basel, Switzerland. This article is an open access article distributed under the terms and conditions of the Creative Commons Attribution (CC BY) license (https://creativecommons.org/licenses/by/4.0/).

Abstract: Metal ion studies in wastewater are required on a regular basis for environmental monitoring and assessment. Less metal ion concentrations and the interference from complex sample matrices remains challenging for instrumental quantification. Herein, we proposed a fix-bed solid phase extraction method, consisting of a newly prepared dimercaptosuccinic acid functionalized polystyrene beads. The ligand forms stable complex with Hg(II), Pb(II), and Cd(II), evident by experimental as well as density functional theory. The metal-ligand stabilization energy calculations, suggested the higher selectivity of polystyrene dimercaptosuccinic acid (PSDMSA) toward Pb(II) compared to Cd(II) and Hg(II). The prepared adsorbent was utilized to enrich Hg(II), Pb(II), and Cd(II) ions from environmental samples. Column parameters were studied in detail and optimized accordingly. The preconcentration factor for Hg(II), Pb(II), and Cd(II) were found to be 900, with the preconcentration limit of 0.74 μg L^{-1}. The detection limit for Pb(II), Cd(II), and Hg(II) ions was found to be 1.3 ± 0.2, 1.5 ± 0.3, and 1.8 ± 0.3 ng L^{-1}, respectively. The method accuracy was tested against systematic and continuous errors by standard addition method (<5% RSD). Real samples was successfully analyzed following the proposed method.

Keywords: toxicity; extraction; trace metal ions; spectroscopy; density functional theory

1. Introduction

Water pollution because of the discharge of heavy metals in various forms into environmental water streams by various industrial sources has grown to be one of many concerns worldwide. Mercury (Hg), lead (Pb), and cadmium (Cd) ranked noxious among all hazards contained in the toxic waste sites at national priority list by the Agency for Toxic Substances and Disease Registry (ASTDR) [1]. The acceptable limits in drinking water for these metal ions are 2, 15, and 5 μg L^{-1}, respectively [2]. These heavy metal ions, alone or in combination, constitute a severe hazard to biota and human health [3–7]. Therefore, environmental monitoring to test their contamination level and assessment of the exposure are one of the top priorities acquiesced by WHO (World Health Organization) [8,9]. It is essential to develop sensitive, accurate, and economical means to analyze environmental water samples [10–14]. Metal–ligand complex formation is of special significance where a specific ligand can selectively coordinate with the heavy metal ions in order to extract

them from the complex sample matrix [3]. In solid phase extraction (SPE), research has been focused on the preparation of new adsorbent materials including polymeric materials, nano-materials, metal-organic framework, and carbonaceous materials for wastewater remediation [15–20]. Polymeric adsorbents has been considered as a promising material, since it has an advantage of column operation over nano-materials, and widely acceptable in water treatment techniques [21–25]. Although several nano-materials have been reported either in the batch mode or column operations [26–30]. However, due to very small size (nm) and high dispersity, the use of nano-materials in column operations may lead to adsorbent leaching during column experiments. Furthermore, the release of nano-materials may cause toxicity to ecosystem [31,32] and requires another developed method for their extraction.

In this work, the authors synthesized a new adsorbent fabricated by the functionalization of chloromethylated polystyrene resin by a dimercaptosuccinic acid (DMSA) ligand in single step (PSDMSA). DMSA, a bidentate ligand possess two carboxylic and two thiol functionality (Figure 1). DMSA selectively binds to heavy metal ions either through the two mercapto groups or one carboxyl and one mercapto group. The sulfur atoms of the thiol groups in DMSA have a higher complexation ability for Hg(II), Pb(II), and Cd(II) ions. The selectivity and coordination mechanism of prepared PSDMSA sorbent for Hg(II), Pb(II), and Cd(II) have been studied via experimental as well as DFT studies and reported in this work. The polystyrene resin with high surface area and porosity after functionalization leads to high selectivity toward the studied metal ions. The prepared PSDMSA sorbent was successfully utilized in the preconcentration of metal ions from the environmental samples.

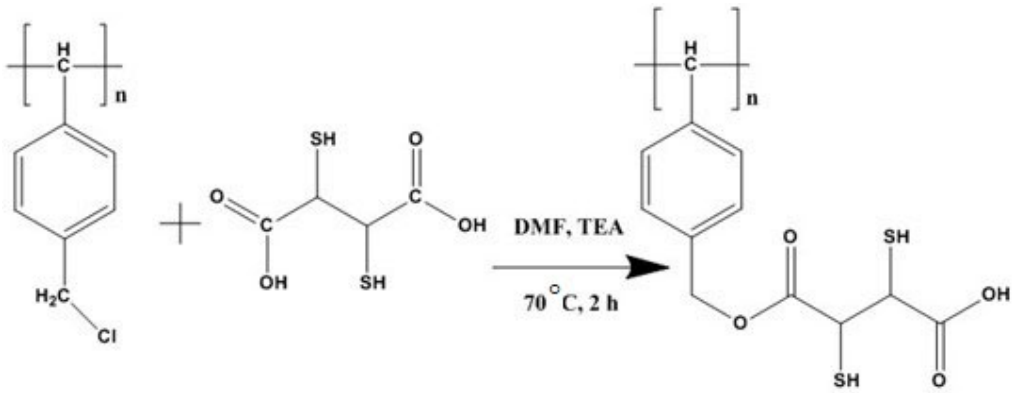


Figure 1. Schematic diagram showing synthesis of PSDMSA. Dimethylformamide (DMF); Triethylamine (TEA).

2. Experimental

2.1. Reagents and Solutions

The resin beads and DMSA were purchased from Merck (Steinheim, Germany). All metal ions solutions used (1000 ppm) was obtained from Merck (Beijing, China). The model solutions of desired concentrations were prepared from stock solution after dilution. All glassware's were dipped overnight in 2% nitric acid solution before use.

2.2. Equipments

The incorporation of ligand was confirmed by the Fourier transformed infrared spectroscopy (FT-IR, Perkin Elmer, Waltham, MA, USA). The elemental constituents was analyzed using energy dispersive X-ray analysis (Bruker, Germany). The surface area measurements was carried out using Quanta chrome equipment (Boynton Beach, FL, USA) using nitrogen gas. A Zetasizer (Malvern Instruments, Malvern, UK) was used to study zeta potential (z). The concentrations of Hg(II), Pb(II) and Cd(II) was analyzed by inductively coupled plasma optical emission spectrophotometer (ICP-OES, Perkin Elmer, Waltham, MA, USA; model Avio 200).

2.3. Computational Studies

The quantum mechanics was applied to compute the geometries, chemical stability, bond lengths, stabilization energies, and binding energies of the free PSDMSA and metal-coordinated PSDMSA and considering water as a solvent. The calculations were performed using the Gaussian 09 software package [33]. For C, O, S, and H elements, the B3 LYP command with the 6-311++G basis set was employed and the LANL2 DZ basis set for metal ions was used [34,35]. The solvent effect was simulated by the conductor polarizable continuum model (CPCM) [36].

2.4. Synthesis of PSDMSA Adsorbent

The chloromethylated polystyrene (PS) beads were chemically functionalized with DMSA ligand by a simple condensation procedure, followed by nucleophile addition to eliminate HCl molecules. In brief, 10.0 g of PS beads was soaked overnight with 50 mL of dimethylformamide (DMF). A 10 mL solution of DMSA (1.5 g), prepared in DMF was added to the PS solution. The whole content was bath sonicated for 15 min to mix the two components. Afterward, the whole components was refluxed (with stirring) for 2.0 h at 70 °C with triethylamine (TEA catalyst) to remove the HCl bi-product. The product was cooled down and filtered off by using a 0.22 µm filter paper. The obtained PSDMSA was sequentially cleaned with DMF, ethanol, and deionized (DI) water to remove the reacted DMSA ligand. The PSDMSA was oven dried at 50 °C for 12 h before further use. The synthesis scheme for single unit is presented in Figure 1.

2.5. Batch Studies

The batch experiment was conducted by equilibrating the 100 mg of PSDMSA adsorbent with individual metal ions (500 ppm) in a 100 mL Erlenmeyer flask, at different sample pH (1–7). The shaking (equilibrium) time for each metal ions was 24 h. Afterward, the concentration of remaining (un-adsorbed) analytes was determined using ICP-OES to measure the uptaken metal ions. The uptaken metal ions at varying sample pH (Figure 2A), were observed by using the given equation:

$$Q_{pH} = \frac{(C_i - C_f) * V}{m} \quad (1)$$

where, C_i and C_f—concentration of loaded and left metal ions (mg L^{-1}), respectively; V-sample volume (L) and m- adsorbent mass (g). The metal ions uptaken capacity of PDMSA was 0.75 for Hg(II), 0.62 for Pb(II) and 0.66 mmol g^{-1} for Cd(II), at optimum pH value of 6.0 ± 0.2.

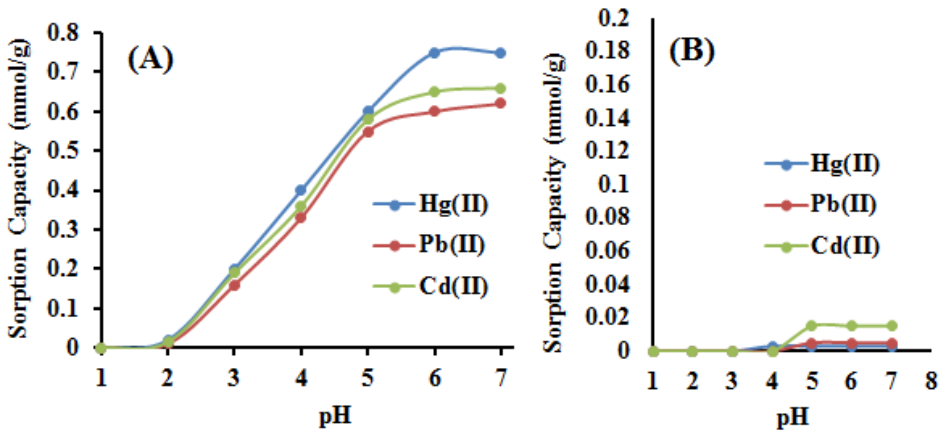


Figure 2. The pH envelop for (**A**) PSDMSA and (**B**) PS sorbent (sample volume 100 mL; sorbent dose 100 mg; sample flow rate 5 mL min^{-1}; eluent volume 3 mL).

In Figure 3 were observed zeta potential studies.

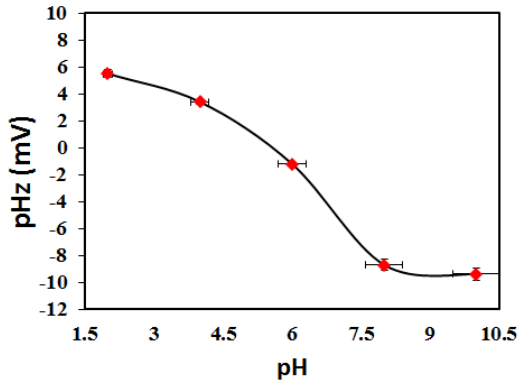


Figure 3. Zeta potential of PSDMSA adsorbent (sample volume 100 mL; sorbent dose 100 mg).

2.6. Column Procedure for Metal Ions Preconcentration

Individual model solution (100 mL) for Hg(II), Pb(II), and Cd(II) ions, at concentration of 10 μg L^{-1}, was set to pH 6.0 ± 0.2. The model solutions was passed through a glass column possess 100.0 mg of PSDMSA adsorbent, at the flow rate of 5 mL min^{-1}, optimized by peristaltic pump (Millipore XI0422050, Beijing, China). The concentration of uptaken metal ions was determined by ICP-OES after elution with 3 mL of 1 M hydrochloric acid.

3. Results and Discussion

3.1. Characterization of PSDMSA

The incorporation of surface functional groups onto PS beads was observed and confirmed by fourier transform infrared spectroscopy (FTIR) analysis. In the FTIR spectra (Figure 4), a peak at 3200–3500 cm^{-1} attributes to presence of –OH group of carboxylic acid of the DMSA ligand. The strong peak at 1700 cm^{-1} confirms to C=O groups. The peak at 1350 cm^{-1} ascertain the C–O stretching. The peak at 2900 cm^{-1} represents the –CH stretching vibrations of aromatic carbon of the PS beads, respectively. The prominent bands obtained at 3250 cm^{-1} and 1025 cm^{-1} are corresponds to –OH and –SH stretching vibrations, and confirm the successful immobilization of ligand. The nitrogen gas adsorption–desorption isotherm is shown in Figure 5. The surface area of PSDMSA, estimated by multipoint BET method, was observed to 44.15 m^2 g^{-1}. The elemental mapping of the prepared PSDMS A after metal ions adsorption was obtained from the energy dispersive X-ray spectroscopy (Figure 6), and depicts the successful adsorption of metal ions.

3.2. Optimized Experimental Variables

3.2.1. Effect of Sample pH

The sample pH is an important parameter for metal-ligand complexation. The effect of sample pH on Hg(II), Pb(II), and Cd(II) adsorption by PSDMSA, was studied by batch adsorption strategy. Details are given in Section 2.4. For comparative studies, a nascent PS was also studied for metal ions adsorption following the same procedure as for PSDMSA. The adsorption trend for PSDMSA is shown in Figure 2. For nascent PS adsorbent, no significant adsorption was observed at all pH values (Figure 2B). The functional groups of PSDMSA gets protonated with positive charge at acidic pH values of 1–2, which reduced the chelating capacity with metal ions. This might be because metal ions repel protonated binding sites electrostatically. However, at higher pH values, the adsorption of metal ions significantly increases with the increase of pH from 3–7. This may be due the dissociation of the H^+ ions, which reduces the positive charge density on functional groups and thus, increases the coordination ability of ligand with the metal ions. This was also observed from zeta potential studies (Figure 3). Another important factor, promoting the metal ions adsorption is Lewis soft-soft interaction. According to Pearson's Hard and Soft acid

base theory Pb(II), Cd(II), and Hg(II) are the soft acids and form favorable complexes with the soft base (thiol groups) of the ligands [37,38]. In conclusion, at optimal pH levels, inner-sphere surface chelation dominates strong metal ion sorption, rather than physical adsorption [39]. Hence, pH 6 was optimized for the adsorption of metal ion in all further experiments. Furthermore, the stability order of metal-PSDMSA complexes is also evidenced by following the theoretical studies.

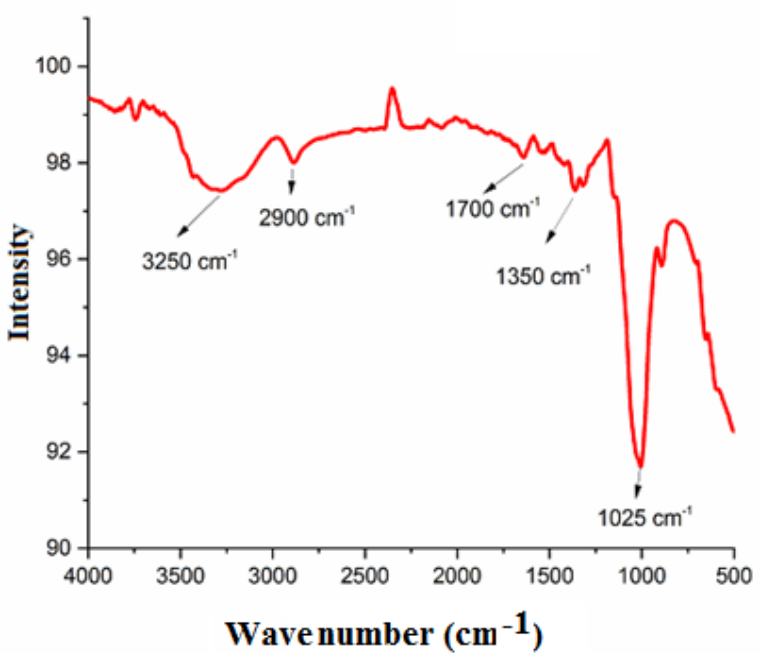


Figure 4. FTIR spectra of PSDMSA.

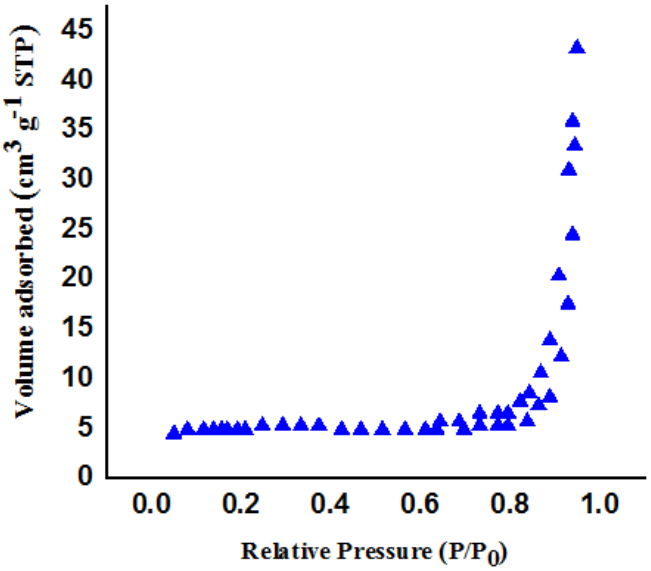


Figure 5. Nitrogen adsorption isotherm of PSDMSA adsorbent.

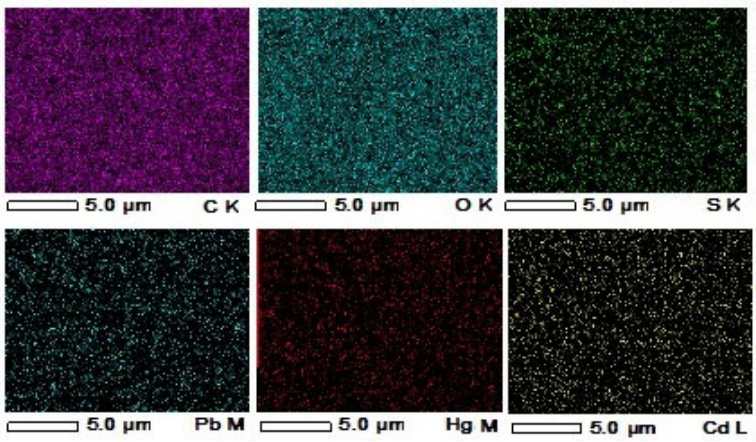


Figure 6. Elemental mapping image of PSDMSA after metal ion adsorption.

3.2.2. Theoretical Validation

The optimized structures of PSDMSA and Me-PSDMSA with their structural parameters are presented in Figures 7 and 8. It is assumed that the PSDMSA forms two possible complexes with metal ions either by one −COOH and one −SH group (complex 1) OR by two -SH groups (complex 2). Only the simplest complexes 1 and 2 were calculated. The tridentate and tetra dentate complexes are not studied in this article. Comparison associated with the bond length of free PSDMSA and metal affiliated complexes reveals that the C-O and C-S bond distances of PSDMSA varies on complex formation (Table 1). Moreover, in Me-PSDMSA complexes the Me-S and Me-O bond lengths for Pb(II), Cd(II), and Hg(II) for both the complexes type are mentioned in Table 1. The obtained data suggest that, in complex 1 and 2, Cd(II) and Hg(II) forms stronger complexes with PSDMSA than Pb(II). Moreover, in complex 1, the average Me-S distances for Pb(II), Cd(II), and Hg(II) complexes are 2.584, 1.521, and 1.521 Å, respectively, which are less than those of average Me-S distances in complex 2. This indicates that the interaction between metal ions and PSDMSA in complex 1 is stronger than complex 2. It is concluded that the carboxylic/thiol groups (Complex 1) have high affinity for metal ion complexation and act as the primary metal ion binding sites in PSDMSA than thiol/thiol groups.

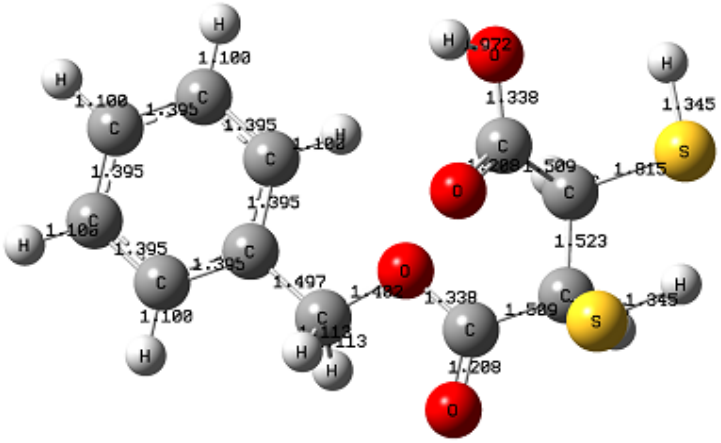


Figure 7. Optimized structure of PSDMSA.

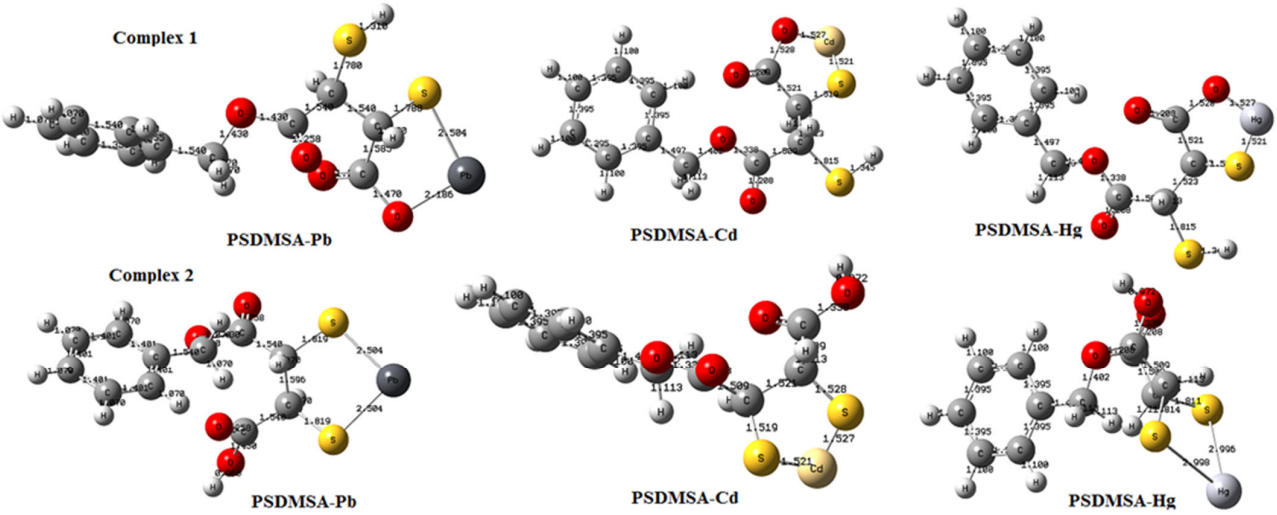


Figure 8. Optimized structures of Me-PSDMSA for complex type 1 and type 2.

Table 1. Optimized structural bond length of PSDMSA and Me-PSDMSA.

	Binding Mode	Bond Length			
		C-S	C-O	Me-S	Me-O
Complex 1	PSDMSA	1.815	1.338	-	-
	Pb-PSDMSA	1.788	1.470	2.584	2.186
	Cd-PSDMSA	1.519	1.528	1.521	1.527
	Hg-PSDMSA	1.519	1.528	1.521	1.527
Complex 2	Pb-PSDMSA	1.819	1.430	2.504	-
	Cd-PSDMSA	1.519	1.338	1.521	-
	Hg-PSDMSA	1.811	1.338	2.996	-

Natural bond order (NBO) analysis was performed to investigate the charge transfer phenomenon between the functional groups of PSDMSA and metal ions during complexation. The binding (E_{bind}) and stabilization energies (E) were calculated and are reported in Table 2. The larger E value of M-L complex represents a higher stability. From Table 2, Pb-PSDMSA complex shows the highest stabilization energy value, suggested the higher selectivity of PSDMSA toward Pb(II) in comparison to Cd(II) and Hg(II).

Table 2. Calculated E(2) and $E_{(bind)}$ energies of PSDMSA-metal complexes.

	Binding Mode	Charge Transfer	E(2)	$E_{(bind)}$
Complex 1	Pb-PSDMSA	LPO→LP*PbLPS→LP*Pb	29.232	−107.865
	Cd-PSDMSA	LPO→LP*CdLPS→LP*Cd	8.288	−36.334
	Hg-PSDMSA	LPO→LP*HgLPS→LP*Hg	5.241	−29.984
Complex 2	Pb-PSDMSA	LPS→LP*PbLPS→LP*Pb	33.416	−118.227
	Cd-PSDMSA	LPS→LP*CdLPS→LP*Cd	21.826	−42.164
	Hg-PSDMSA	LPS→LP*HgLPS→LP*Hg	13.901	−35.603

3.2.3. Optimized Flow Rate

A sample solution (50 mL) with 10 µg of each metal ion was run at varied sample flow rates of 2–10 mL min^{-1} to optimize the column flow rate for metal ion adsorption. Figure 9 shows that the adsorption of Pb(II), Cd(II), and Hg(II) were accomplished satisfactorily up to a sample flow rate of 5 mL min^{-1}. When the sample flow was increased to 6–8 mL min^{-1}, there was a 6–10% drop in Pb(II) adsorption and an 8–15% decrease in Cd(II) and Hg(II) adsorption. The reduction in metal ion adsorption with increased sample flow might be attributed to shorter chelation time for the metal-ligand coordination. As a result, 5 mL min^{-1} of sample flow was optimized and used for sample analysis.

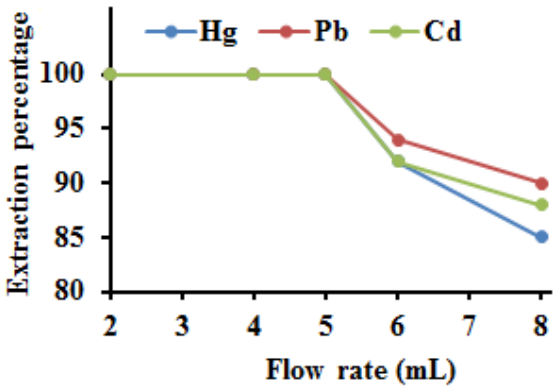


Figure 9. Effect of sample flow rate (volume 50 mL; metal ions 10 µg; sample pH 6; eluent volume 3 mL).

3.2.4. Co-Ions Interferences and Desorption Studies

In the preconcentration of analyte metal ions, associated co-existing ions such as alkali and alkaline earth metals often interfere. They might compete with metal ions and interfere in the complexation reaction, thereby reducing the analyte adsorption. Moreover, these concomitants along with analyte ions cause the interference in the instrumental analysis. The ionic concentrations varied >±5% in the preconcentration of analyte ions were considered to be the interferents. Aliquots (100 mL) containing individual metal ion (10 µg) and high concentrations of concomitants were tested. The adsorbed metal ions were eluted and sequentially analyzed by ICP-OES. Results are shown in (Table 3). It was observed that the percent recovery of analytes are well above 96%, indicating that there were no significant interferences by concomitants in the analysis of target ions.

Desorption of metal ions from column bed was performed using HCl and HNO_3 with varying concentrations (0.5–2.0) and volumes (1–5 mL). We found that 1 M HCl (3 mL) would completely elute the Pb(II), Cd(II) and Hg(II) ions, from the column bed with >99% extraction. Therefore, 3 mL of 1 M HCl was optimized for stripping of metal ions.

Table 3. Analytical data for interference studies (volume 100 mL; pH 6; metal ion 10 µg; PSDMSA amount 100 mg; flow rate 5 mL min^{-1}; eluent volume 3 mL).

Foreign Ions	Co-Ions Added ($\times 10^3$ µg L^{-1})	Recovery % (RSD) [a]		
		Hg(II)	Pb(II)	Cd(II)
CO_3^{2-}, SO_4^{2-}, PO_4^{2-}, NO_3^-	400	97.5 (1.25)	96.1 (1.96)	97.2 (1.88)
Cl^-, Br^-	650	98.5 (2.27)	97.1 (2.16)	99.6 (2.73)
Na^+, K^+, Ca^{2+}, Mg^{2+}	600	98.5 (1.86)	99.6 (2.14)	98.3 (2.19)
Co^{2+}, Ni^{2+}, Cu^{2+}, Zn^{2+}	150	96.8 (2.25)	97.5 (3.12)	97.3 (3.25)

[a] N = 3.

3.2.5. Preconcentration Studies

Samples with varying sizes (1500, 2000, 2500, 2700, 3000, and 3200 mL at pH 6.0) containing 2 µg of individual metal ions were flowed through PSDMSA packed column at a flow rate of 5 mL min^{-1}. The effluent collected was discarded. The adsorbed metal ions was eluted and the concentration of metal ions was analyzed by ICP-OES. From the obtained data it was found that Pb(II), Cd(II), and Hg(II) ions were quantitatively recovered up to a sample volume of 3000 mL with metal ions recovery of 99.0 ± 5%, therefore, suggesting a preconcentration limit of 0.74 µg L^{-1}, with the preconcentration factor of 900 (2700 mL sample divided by 3 mL eluent). At sample volume of 3000 mL, the analyte adsorption was reduced to 92% for Pb(II) and Cd(II) and 85% for Hg(II). Because of the increased preconcentration factor, the adsorbent might be used with any detection approach, whether offline or online. The presence of a high number of hydrophilic groups

on the adsorbent increased the preconcentration factor by making it easier to achieve equilibrium between active sites and metal ions in aqueous solutions.

3.3. Analytical Figures of Merits

After the preconcentration operation, the calibration plots were linear in the range of 0.01–100 μg L^{-1}. The correlation coefficient (R^2) obtained was at least 0.999. To ensure accuracy, the standard addition procedure was used. With a RSD (relative standard deviation) value of 3.5–5%, the recovery of spiked amounts (Pb, Cd, Hg) were close to 99.9%. Table 4 displays the findings. At a 95% confidence level, the Student's *t*-test values determined here, were found smaller than the critical *t* values (4.303, $n = 5$) (Table 4). Five repeated analysis with 5 μg of analyte ions with 50 mL solutions were used to validate the method's accuracy. The method's accuracy is shown by the lower value of coefficients of variation (5%). The slope of the calibration curves is referred to as sensitivity. The method LOD (limit of detection) for Pb(II), Cd(II), and Hg(II) ions, calculated as 3s/m (s- standard deviation; m slope), were determined to be 1.3 ± 0.2, 1.5 and 1.8 ± 0.3 ng L^{-1}, respectively.

Table 4. Analysis of real samples after column preconcentration (volume 100 mL; pH 6; PSDMSA amount 100 mg; flow rate 5 mL min^{-1}; eluent 3 mL of 1 M HCl).

Samples	Analyte	Value after Preconcentration [a] (μg L^{-1})	Amount Spiked (μg)	Amount Found [b]	Value of *t*-Test	% Recovery
River Water	Hg(II)	2.8 ± 0.07	5	7.7 ± 0.52	0.48	98.7
			10	12.8 ± 0.41	0.55	100
	Pb(II)	5.6 ± 0.13	5	10.6 ± 0.89	0.75	100
			10	15.45 ± 1.13	0.82	99.0
	Cd(II)	3.7 ± 0.05	5	8.66 ± 0.58	1.17	99.5
			10	13.68 ± 0.45	0.43	99.8
Electroplating Wastewater	Hg(II)	18.6 ± 0.83	5	23.5 ± 1.4	1.04	98.8
			10	28.6 ± 1.8	0.95	100
	Pb(II)	24 ± 0.81	5	28.8 ± 0.7	1.34	99.3
			10	34.0 ± 1.5	2.11	100
	Cd(II)	28 ± 0.82	5	32.7 ± 0.84	1.88	99.0
			10	38.1 ± 1.81	1.96	100.2
Tap Water	Hg(II)	Not detected	5	5.0 ± 0.73	1.56	100
			10	10.02 ± 0.98	0.88	100.2
	Pb(II)	Not detected	5	5.0 ± 0.3	0.85	100
			10	10.2 ± 0.1	0.49	102
	Cd(II)	Not detected	5	5.1 ± 0.43	1.45	102
			10	10.0 ± 1.91	1.41	100

[a] Mean value ± standard deviation; [b] μg g^{-1}; N = 3.

3.4. Application of the Method

Three environmental samples were subjected to the devised preconcentration method. The sorbed metal ions were eluted and examined by ICP-OES after preconcentration. Table 4 shows the amounts of Pb(II), Cd(II), and Hg(II) measured in genuine samples. The analytes that were retained were analyzed with a 95% confidence interval. With a RSD of 3.5–4.5%, the mean percent recoveries vary from 98.7–102%. With an average error of 3%, the new method demonstrated high repeatability.

4. Conclusions

We proposed a new SPE column packed with thiol-immobilized polystyrene grains for the selective extraction of metal ions. The sorption behaviors of the prepared sorbent was evaluated for toxic metal ions. The sorbent shows efficient and fast sorption behavior in aqueous solutions. The proposed method shows the fair preconcentration limit of 0.74 μg L^{-1}, for Hg(II), Pb(II), and Cd(II). The metal ions sorption mechanism was revealed by studying the effect of sample pH. The E_{bind} value for Pb(II) (−118.227 Kcal mol^{-1}) was

higher than the E_{bind} of Cd(II) (−42.164 Kcal mol^{-1}) and Hg(II) (−35.603 Kcal mol^{-1}), suggesting that the PSDMSA forms more stable complex with Pb(II) compared to Cd(II) and Hg(II) ions. A comparative data of this study with other reported methods has been provided in Table 5, to make the manuscript potential for the valued readers. The obtained results highlights the usefulness of surface functionalization and expands the potential applicability of the prepared column for selective extraction and routine analysis of toxic metal ions from real samples.

Table 5. Comparative analytical data of presented work with other recent reports.

Adsorbent	Metal Ions	Method	Preconcentration Limit	Preconcentration Factor (μg L^{-1})	Ref.
PSDMSA	Pb; Cd; Hg	SPE/ICP-OES	0.74	900	This work
GO-APA	Pb; Cd; Cu	SPE/ICP-OES	0.45; 0.45; 0.40	733; 733; 833	[40]
APBC	Cu; Pb; Cd	SPE/ICP-OES	0.34; 0.37; 0.37	580; 540; 540	[41]
XAD-4	Cu; Ni; Pb	SPE/ICP-OES	0.31; 0.42; 0.43	Not reported	[42]
F-CNT	Pb	SPE/FAAS	1.2	94	[43]
MNPC	Pb; Cd	SPE/ICP-MS	0.49; 3.1	Not reported	[44]

Author Contributions: Conceptualization, H.A.; formal analysis, S.G.A. and H.M.K.; investigation, K.U.; project administration, A.A.; software, U.H.; writing—original draft, H.A.; writing—review and editing, K.U. All authors have read and agreed to the published version of the manuscript.

Funding: This research was funded by Taif University Research Supporting Project, grant number "TURSP-2020/124" and "The APC was funded by Taif University Research Supporting Project".

Institutional Review Board Statement: Not applicable.

Informed Consent Statement: Not applicable.

Acknowledgments: Abuzer Ali is thankful to Taif University Researchers Supporting Project Number (TURSP-2020/124), Taif University, Taif, Saudi Arabia.

Conflicts of Interest: The authors declare no conflict of interest.

References

1. Agency for Toxic Substances and Disease Registry. Available online: https://www.atsdr.cdc.gov/spl/index.html#2019spl (accessed on 28 August 2021).
2. Environmental Protection Agency. Available online: https://www.epa.gov/ground-water-and-drinking-water/national-primary-drinking-water-regulations#Inorganic (accessed on 28 August 2021).
3. Rayner-Canham, G.; Overton, T. *Descriptive Inorganic Chemistry*; Macmillan: New York, NY, USA, 2009.
4. Chen, X.C.; Zhu, X.H.; Lin, B.G.; Li, L.Z.; Yu, Z.L.; Xiang, M.D.; Yu, Y.J. Children's non-carcinogenic health risk assessment of heavy metals exposure to residential indoor dust around an e-waste dismantling area in South China. *Zhonghua Yu Fang Yi Xue Za Zhi* **2019**, *53*, 360–364.
5. Chen, M.-L.; Sun, Y.; Huo, C.-B.; Liu, C.; Wang, J.-H. Akaganeite decorated graphene oxide composite for arsenic adsorption/removal and its proconcentration at ultra-trace level. *Chemosphere* **2015**, *130*, 52–58. [CrossRef]
6. Dong, W.; Zhang, Y.; Quan, X. Health risk assessment of heavy metals and pesticides: A case study in the main drinking water source in Dalian, China. *Chemosphere* **2019**, *242*, 125113. [CrossRef]
7. Kicinska, A. Environmental risk related to presence and mobility of As, Cd and Tl in soils in the vicinity of a metallurgical plant -Long-term observations. *Chemosphere* **2019**, *236*, 124308. [CrossRef]
8. Yan, H.-X.; Kong, D.-D.; Li, X.-Y.; Fan, Z.-W.; Yang, M.-H. Pollution level and health risk assessment of heavy metals and hazardous elements in Bombyx Batryticatus. *Zhongguo Zhong Yao Za Zhi* **2019**, *44*, 5051–5057. [PubMed]
9. WHO. Drinking Water, Fact Sheet No. 391. Media Centre. Available online: http://www.who.int/mediacentre/factsheets (accessed on 28 August 2021).
10. Topuz, B. Simultaneous Spectrometric Determination of Cu(II), Co(II), and Ni(II) in Pharmaceutical and Environmental Samples with XAD-4/DMMDTC Solid-Phase Extraction System. *Biol. Trace Elem. Res.* **2020**, *194*, 295–302. [CrossRef]
11. Lei, C.; Gao, J.; Ren, W.; Xie, Y.; Abdalkarim, S.Y.H.; Wang, S.; Ni, Q.; Yao, J. Fabrication of metal-organic frameworks@cellulose aerogels composite materials for removal of heavy metal ions in water. *Carbohydr. Polym.* **2018**, *205*, 35–41. [CrossRef]
12. Liu, Z.; Wang, H.; Liu, C.; Jiang, Y.; Yu, G.; Mu, X.; Wang, X. Magnetic cellulose–chitosan hydrogels prepared from ionic liquids as reusable adsorbent for removal of heavy metal ions. *Chem. Commun.* **2012**, *48*, 7350–7352. [CrossRef] [PubMed]

13. Kumar, V.; Parihar, R.; Sharma, A.; Bakshi, P.; Sidhu, G.P.S.; Bali, A.S.; Karaouzas, I.; Bhardwaj, R.; Thukral, A.; Gyasi-Agyei, Y.; et al. Global evaluation of heavy metal content in surface water bodies: A meta-analysis using heavy metal pollution indices and multivariate statistical analyses. *Chemosphere* **2019**, *236*, 124364. [CrossRef]
14. Li, H.; Dai, Q.; Yang, M.; Li, F.; Liu, X.; Zhou, M.; Qian, X. Heavy metals in submicronic particulate matter (PM1) from a Chinese metropolitan city predicted by machine learning models. *Chemosphere* **2020**, *261*, 127571. [CrossRef] [PubMed]
15. Schmitz, T.C.; Eren, A.D.; Spierings, J.; de Boer, J.; Ito, K.; Foolen, J. Solid-phase silica-based extraction leads to underestimation of residual DNA in decellularized tissues. *Xenotransplantation* **2020**, *28*, e12643. [CrossRef] [PubMed]
16. Moradi Shahrebabak, S.; Saber-Tehrani, M.; Faraji, M.; Shabanian, M.; Aberoomand-Azar, P. Magnetic solid phase extraction based on poly(beta-cyclodextrin-ester) functionalized silica-coated magnetic nanoparticles (NPs) for simultaneous extraction of the malachite green and crystal violet from aqueous samples. *Environ. Monit. Assess.* **2020**, *192*, 1–13. [CrossRef]
17. Kojidi, M.H.; Aliakbar, A. Synthesis of graphene oxide-based poly(p-aminophenol) composite and its application in solid phase extraction of trace amount of Ni(II) from aquatic samples. *Environ. Monit. Assess.* **2019**, *191*, 145. [CrossRef]
18. Liu, X.; Ma, R.; Wang, X.; Ma, Y.; Yang, Y.; Zhuang, L.; Zhang, S.; Jehan, R.; Chen, J.; Wang, X. Graphene oxide-based materials for efficient removal of heavy metal ions from aqueous solution: A review. *Environ. Pollut.* **2019**, *252*, 62–73. [CrossRef] [PubMed]
19. Francisco, J.E.; Feiteira, F.N.; Da Silva, W.A.; Pacheco, W. Synthesis and application of ion-imprinted polymer for the determination of mercury II in water samples. *Environ. Sci. Pollut. Res.* **2019**, *26*, 19588–19597. [CrossRef]
20. Li, B.; Chen, Z.; Li, Y.; Yang, W.; Wang, W. Visualization analysis of graphene and its composites for heavy metal wastewater applications. *Environ. Sci. Pollut. Res.* **2019**, *26*, 27752–27760. [CrossRef]
21. Liu, F.; Zhang, X.; Shan, C.; Pan, B. Effect of 3-D distribution of ZVI nanoparticles confined in polymeric anion exchanger on EDTA-chelated Cu(II) removal. *Environ. Sci. Pollut. Res.* **2019**, *26*, 10013–10022. [CrossRef]
22. Chen, D.; Wang, L.; Ma, Y.; Yang, W. Super-adsorbent material based on functional polymer particles with a multilevel porous structure. *NPG Asia Mater.* **2016**, *8*, e301. [CrossRef]
23. Kim, S.; Lee, T.G. Removal of Cr(VI) from aqueous solution using functionalized poly(GMA-co-EGDMA)-graft-poly(allylamine). *React. Funct. Polym.* **2018**, *134*, 133–140. [CrossRef]
24. Zhu, F.; Li, L.; Li, N.; Liu, W.; Liu, X.; He, S. Selective solid phase extraction and preconcentration of Cd(II) in the solution using microwave-assisted inverse emulsion-suspension Cd(II) ion imprinted polymer. *Microchem. J.* **2021**, *164*, 106060. [CrossRef]
25. Dahaghin, Z.; Mousavi, H.Z.; Boutorabi, L. Application of magnetic ion-imprinted polymer as a new environmentally-friendly nonocomposite for a selective adsorption of the trace level of Cu(II) from aqueous solution and different samples. *J. Mol. Liq.* **2017**, *243*, 380–386. [CrossRef]
26. Wang, L.; Wu, X.-L.; Xu, W.-H.; Huang, X.-J.; Liu, J.-H.; Xu, A.-W. Stable Organic–Inorganic Hybrid of Polyaniline/α-Zirconium Phosphate for Efficient Removal of Organic Pollutants in Water Environment. *ACS Appl. Mater. Interfaces* **2012**, *4*, 2686–2692. [CrossRef]
27. Cheng, W.; Rechberger, F.; Niederberger, M. Three-Dimensional Assembly of Yttrium Oxide Nanosheets into Luminescent Aerogel Monoliths with Outstanding Adsorption Properties. *ACS Nano* **2016**, *10*, 2467–2475. [CrossRef]
28. Li, J.-R.; Wang, X.; Yuan, B.; Fu, M.-L.; Cui, H.-J. Robust removal of heavy metals from water by intercalation chalcogenide [CH3NH3]2xMnxSn3−xS6·0.5H2O. *Appl. Surf. Sci.* **2014**, *320*, 112–119. [CrossRef]
29. Gao, M.-R.; Xu, Y.-F.; Jiang, J.; Yu, S.-H. Nanostructured metal chalcogenides: Synthesis, modification, and applications in energy conversion and storage devices. *Chem. Soc. Rev.* **2013**, *42*, 2986–3017. [CrossRef] [PubMed]
30. Li, J.-R.; Wang, X.; Yuan, B.; Fu, M.-L. Layered chalcogenide for Cu2+ removal by ion-exchange from wastewater. *J. Mol. Liq.* **2014**, *200*, 205–212. [CrossRef]
31. Elsaesser, A.; Howard, C.V. Toxicology of nanoparticles. *Adv. Drug Deliv. Rev.* **2012**, *64*, 129–137. [CrossRef]
32. Buchman, J.T.; Hudson-Smith, N.V.; Landy, K.M.; Haynes, C.L. Understanding Nanoparticle Toxicity Mechanisms to Inform Redesign Strategies to Reduce Environmental Impact. *Acc. Chem. Res.* **2019**, *52*, 1632–1642. [CrossRef]
33. Becke, A.D. Density-functional exchange-energy approximation with correct asymptotic behavior. *Phys. Rev. A* **1988**, *38*, 3098–3100. [CrossRef]
34. Lee, C.; Yang, W.; Parr, R.G. Development of the Colle-Salvetti correlation-energy formula into a functional of the electron density. *Phys. Rev. B* **1988**, *37*, 785–789. [CrossRef]
35. Becke, A.D. Density-functional thermochemistry. V. Systematic optimization of exchange-correlation functionals. *J. Chem. Phys.* **1997**, *107*, 8554–8560. [CrossRef]
36. Tomasi, J.; Mennucci, B.; Cammi, R. Quantum Mechanical Continuum Solvation Models. *Chem. Rev.* **2005**, *105*, 2999–3094. [CrossRef]
37. Pearson, R.G. Hard and soft acids and bases, HSAB, part 1: Fundamental principles. *J. Chem. Educ.* **1968**, *45*, 581. [CrossRef]
38. Pearson, R.G. Hard and soft acids and bases, HSAB, part II: Underlying theories. *J. Chem. Educ.* **1968**, *45*, 643. [CrossRef]
39. Rabinovich, D. Descriptive Inorganic Chemistry (Rayner-Canham, Geoff). *J. Chem. Educ.* **1998**, *75*, 697. [CrossRef]
40. Ahmad, H.; Husain, F.M.; Khan, R.A. Graphene oxide lamellar membrane with enlarged inter-layer spacing for fast preconcentration and determination of trace metal ions. *RSC Adv.* **2021**, *11*, 11889–11899. [CrossRef]
41. Ahmad, H.; Alharbi, W.; BinSharfan, I.I.; Khan, R.A.; Alsalme, A. Aminophosphonic Acid Functionalized Cellulose Nanofibers for Efficient Extraction of Trace Metal Ions. *Polymers* **2020**, *12*, 2370. [CrossRef]

42. Ozdemir, S.; Kılınç, E.; Acer, Ö.; Soylak, M. Simultaneous preconcentrations of Cu(II), Ni(II), and Pb(II) by SPE using E. profundum loaded onto Amberlite XAD-4. *Microchem. J.* **2021**, *171*, 106758. [CrossRef]
43. Bajaj, S.; Jain, V.; Sharma, N.; Tiwari, S.; Saxena, R. Efficient lead preconcentration using two chemically functionalized carbon nanotubes in hyphenated flow injection-flame atomic absorption spectrometry system. *J. Chromatogr. A* **2021**, *1638*, 461888. [CrossRef] [PubMed]
44. Xu, C.; Peng, C.; He, M.; Chen, B.; Hu, B. Magnetic N-doped porous carbon for analysis of trace Pb and Cd in environmental water by magnetic solid phase extraction with inductively coupled plasma mass spectrometry. *Spectrochim. Acta Part B At. Spectrosc.* **2021**, *184*, 106273. [CrossRef]